https://doi.org/10.5194/egusphere-2023-2735
Preprint. Discussion started: 7 December 2023

Decoupling of δ^{18}O from surface temperature in Antarctica in an ensemble of Historical simulations

Sentia Goursaud Oger[1,2], Louise C. Sime[2], and Max Holloway[3]

[1]CEA/DAM/DIF, Arpajon, France
[2]Ice Dynamics and Paleoclimate, British Antarctic Survey
[3]Scottish Association for Marine Science, Oban, UK

Correspondence: Sentia Goursaud Oger (sentia.oger@cea.fr)

Abstract. Water stable isotopes recorded in Antarctic ice cores have traditionally been used to infer past surface air temperatures (SAT). During the historical period (1850 onward), observational data and good quality ice core records overlap, yielding an opportunity to investigate key relationships between ice core stable water isotope (δ^{18}O) measurements and the Antarctic climate. We present a new ensemble of climate model simulations covering 1851-2004 using the UK Met Office HadCM3 general circulation model equipped with water stable isotopes. Our ensemble captures observed historical SAT and precipitation trends, and weak δ^{18}O trends. The weak δ^{18}O trends mean there is no significant relationship between SAT and δ^{18}O over one third of Antarctica, and also half of our considered ice core sites, though relationships are stronger when using regional averages. The strongest regional relationships occur in the West Antarctic Ice Sheet (WAIS) region. This decoupling between SAT and δ^{18}O occurs primarily because of the impact of autumnal sea ice loss during the simulated warming. The warming and sea ice loss is associated with: (i) changes in near-coastal air mass intrusions (synoptic effects) induced by changes in the large-scale circulation and/or sea ice; (ii) direct sea ice driven changes in moisture pathways (especially lengths) to Antarctica; and (iii) precipitation seasonality changes, again mostly driven by sea ice changes. Consequently when reconstructing temperatures over these timescales, changes in sea ice need to be considered; both to determine the most appropriate SAT and δ^{18}O relationship, and to understand how uncertainties affect the inference of past temperature from ice cores δ^{18}O measurements.

1 Introduction

Strong visible signs of Antarctic response to climate change have recently emerged. While a new sea ice cover minimum was recorded in February 2022 (Raphael and Handcock, 2022; Turner et al., 2022), with an extent of 1.97 million square kilometers, this record was broken the following year with sea ice extent falling to 1.91 million square kilometers on February 13th, 2023, associated with strong westerly winds and a 1.5 °C positive anomaly for Antarctic Peninsula air temperatures. The collapse of Antarctic ice shelves have similarly increased in frequency (Graham et al., 2022; Milillo et al., 2022; Wille et al., 2022), with a 1,600 square kilometers iceberg breaking away from the Brunt ice shelf on January 22nd, 2023. The consequent weakening of the buttressing force from the sea-ice free areas, and ice shelf collapse, acts to accelerate Antarctic ice loss. Thus warming of Antarctica will have significant consequences for global, and regional mean sea level (Edwards et al., 2021; Seroussi et al.,

https://doi.org/10.5194/egusphere-2023-2735
Preprint. Discussion started: 7 December 2023

2020; Parsons et al., 2020; Garbe et al., 2020), alongside consequences for Antarctic life and its environs (Golledge et al., 2019; Post et al., 2019), which require thought about adaptation (Pörtner et al., 2022).

The remote nature of this vast continent means that observational data covering Antarctica are sparse in both space and time (Turner et al., 2004). The reconstruction of past temperature change is thus of paramount importance for understanding natural variability, versus effects in response to anthropogenic climate change. Our understanding of pre-industrial climate change and its variability is mostly based on the reconstruction of temperature from proxy data (Pag, 2019). In Antarctica, water stable isotopes are the measurement most commonly used to reconstruct past surface air temperatures (SAT). This type of reconstruction is generally based on an empirical relationship between present day (PD) surface snow water isotopes and surface air temperature (Dansgaard, 1953). The relationship between SAT and the ratio of heavy water to light water isotopes (expressed as δ^{18}O) from Antarctic surface snow is usually assumed to be linear. When this linear relationship is used to estimate past SAT values from ice core water isotope measurements, it is sometimes referred as the 'ice core paleothermometer' (Lorius and Merlivat, 1977; Masson et al., 2000).

The paleothermometer approach has been successfully applied to deep ice cores to reconstruct past temperatures on long timescales (Jouzel et al., 2007; Lambert et al., 2008; Masson-Delmotte et al., 2010; Wolff et al., 2010). Casado et al. (2023) recently reconstructed the past 1000 year temperature record using an isotope to temperature conversion. This ice core based record was then used to show that simulated temperatures from the Atmospheric General Circulation (AGCM) models run in the frame of the Coupled Model Intercomparison Project Phases 5 (Taylor et al., 2012) and 6 (Eyring et al., 2016, CMIP6) are too low. However, the paleothermometer relationship has been shown to vary spatially over the Antarctic continent (e.g. Sime et al., 2008, 2009a). Goosse et al. (2012); Smerdon et al. (2015) and Neukom et al. (2018) show that noise and the spatial coverage of δ^{18}O and other proxy data affect our understanding of these variations, while Goursaud et al. (2018, 2019) and others show smaller, or less reliable, changes in δ^{18}O for a given temperature change in coastal regions (Isaksson and Karlén, 1994; Sime et al., 2008, 2009a; Abram et al., 2013; Thomas et al., 2013; Goursaud et al., 2017). Data to investigate SAT-δ^{18}O relationships are sparse (Masson-Delmotte et al., 2008; Landais et al., 2017), nevertheless the PAGES 2k Network Antarctica 2k helped to address this question of geographical variations in the SAT-δ^{18}O relationship, by defining regions and compiling the available δ^{18}O data from ice cores (Stenni et al., 2017).

The geographical variability in the 'paleothermometer' is due to controls on δ^{18}O other than SAT. These other controls include: changes related to atmospheric dynamics, such as changes in the synoptic and seasonal nature of precipitation (van Ommen and Morgan, 1997; Krinner and Werner, 2003; Jouzel et al., 2003; Sime et al., 2008) and air mass sources (Landais et al., 2021), various impacts from changes in Antarctic ice sheet morphology (Holloway et al., 2016; Werner et al., 2018; Goursaud et al., 2021), and sea ice variability (Holloway et al., 2018). The stability of the SAT-δ^{18}O relationship has thus been of much of interest for more than two decades (Jouzel et al., 2003). Following Sime et al. (2008) and Sime et al. (2009a), the importance of changes in synoptic events, in the context of the anthropogenic warming, was recently explored by Wille et al. (2019) and Pohl et al. (2021), who confirm that the impact of synoptic changes on the SAT–δ^{18}O relationship can be important for the past paleothermometer during warm climates (Dalaiden et al., 2020).

https://doi.org/10.5194/egusphere-2023-2735
Preprint. Discussion started: 7 December 2023

AGCMs equipped with water stable isotopes are a key tool to investigate the climate processes driving temporal variability in the paleothermometer relationship (e.g. Werner et al., 2001; Sime et al., 2008; Werner et al., 2018). AGCM isotopic studies have focused on the effects of external forcing on the SAT–δ^{18}O relationship, including elevation and greenhouse gases across a range of timescales (e.g. Sime et al., 2009b; Werner et al., 2018; Goursaud et al., 2021). A major result is that, for differing time-scales and driving mechanisms, different SAT–δ^{18}O relationships can be obtained. This emphasises the importance of investigating the impact of atmospheric dynamical drivers, particularly changes in sea ice and precipitation seasonality during past warm periods in Antarctica (Sime et al., 2008, 2009b; Holloway et al., 2016). Only one AGM study has investigated the signature of water stable isotopes in Historical simulations (Yoshimura et al., 2008). While the applicability of the Antarctic paleothermometer relationship has been so investigated across various timescales, it has not yet been thoroughly investigated over the historical period. Furthermore, it has not been investigated using transient Historical (1851-2004) simulations.

Here, we run an ensemble of transient Historical (1851-2004) simulations, using the water stable isotope enabled coupled general circulation model, HadCM3. This ensemble provides a benchmark of Historical precipitated water stable isotopes covering the whole continent, and allows the SAT–δ^{18}O relationship over the Historical period to be investigated. Firstly, we examine trends in SAT, precipitation and δ^{18}O, and compare these against observed trends. We then examine SAT–δ^{18}O relationships, including regional patterns, and the question of model dependence. Finally, in order to understand the drivers of δ^{18}O change, we perform a detrended composite analysis for cold and warm year ensembles, and quantify the impact of seasonality changes in precipitation and δ^{18}O. This analysis provides understanding of SAT–δ^{18}O variability and, in particular, the role of sea ice change during the Historical period on this relationship.

2 Materials and Methods

2.1 Model and simulations

The Historical simulation protocol was defined in the frame of the CMIP Phase 6 (Eyring et al., 2016), with an express purpose to investigate the anthropogenic forcing on climate (Johns et al., 2003) and serve as a benchmark to evaluate model performance (Andrews et al., 2020; Miller et al., 2021; Parsons et al., 2020; Rong et al., 2021; Roach et al., 2020). There have been few examples of studies using Historical simulations focused over Antarctica (Gao et al., 2021; Purich and England, 2021; Raphael et al., 2020; Roach et al., 2020).

Here, we use the Hadley Center general circulation model (HadCM3; GCM), to run six transient Historical simulations. HadCM3 is a version of the coupled Atmosphere-Ocean UK Met Office climate model (Pope et al., 2000; Gordon et al., 2000). The model is equipped with water stable isotopes (Tindall et al., 2009). Its horizontal resolution is 3.75° × 2.5°, and there are 19 vertical levels (Pope et al., 2000; Gordon et al., 2000; Tindall et al., 2009). Our simulations use historical orbital, volcanic and solar forcing following Schurer et al. (2014). We analyse HadCM3 surface air temperature (SAT, °C), precipitation (P, mm/month), precipitation weighted δ^{18}O (δ^{18}O), and sea ice extent (defined as the region of ice-covered ocean, where the sea-ice concentration is $>$15%). HadCM3 provides a reasonable representation of Antarctic climate and δ^{18}O (Turner et al., 2006; Tindall et al., 2009; Holloway et al., 2016).

https://doi.org/10.5194/egusphere-2023-2735
Preprint. Discussion started: 7 December 2023

2.2 Data and methods

We perform a model-data comparison using the Stenni et al. (2017) ice core data compiled by the PAGES A2k project by binning our model output, including δ^{18}O, into 5-years equivalent averages and compute anomalies relative to the 1960-1990 mean. In order to investigate the historical mean climate state and variability, we compute ensemble mean values, covering the period 1851-2004 using monthly outputs. Trends over the whole period, as well as for the last 50 years, are calculated using linear regressions. Where we regress climate variables against δ^{18}O, the linear regressions are computed using the stacked individual ensemble members, rather than using the ensemble mean. This approach ensures that the ensemble variability is included in our linear regression statistics. Gradients from the linear regressions are provided with a plus/minus standard error. Results from linear relationships are stated only where they are significant, using a p-value $\leq$0.05. Our Historical SAT–δ^{18}O linear relationship at the regional scale, as well as at the nearest model grid-cell to each ice core location, are compared with the ECHAM5-wiso slopes and correlation coefficients provided in Stenni et al. (2017).

Composites are used to interpret our results. Warm and cold (versus mean) mean annual composites results are defined using detrended annual area-weighted SAT. The years of the ensemble mean with SAT below (above) the mean minus (plus) one standard deviation constitute a cold (warm) ensemble.

To examine the impact of changing seasonality over the Historical period, we isolate the impact of precipitation and δ^{18}O seasonal changes, recorded in the ensemble mean, on the precipitation weighted δ^{18}O between the first 50 years of the simulation and the last 50 years of the simulations (c.f. Liu and Battisti, 2015; Holloway et al., 2016; Sime et al., 2019). This is calculated as:

$$\Delta^{18}O_{seas} = \frac{\sum_j \delta^{18}O_j^{recent} \times P_j}{\sum_j P_j} - \frac{\sum_j \delta^{18}O_j \times P_j}{\sum_j P_j} \quad (1)$$

$$P_{seas} = \frac{\sum_j \delta^{18}O_j \times P_j^{recent}}{\sum_j P_j^{recent}} - \frac{\sum_j \delta^{18}O_j \times P_j}{\sum_j P_j} \quad (2)$$

The summations, with index j, are over the 12 months of the year. Variables with superscript "recent" indicate that they were extracted for the last 50 years of the simulation whereas the variables without superscript indicate that the variables were extracted for the first 50 years of the simulation.

3 Trends in Antarctic SAT, precipitation, sea ice and δ^{18}O

We analyse our simulations against available observations and reanalysis data at the Antarctic wide-scale before evaluating regional scale climate changes. This is followed by a comparison of simulated δ^{18}O changes against the Stenni et al. (2017) ice core dataset. We note that all trends outlined below are similar regardless of whether we use the full Historical period, or

https://doi.org/10.5194/egusphere-2023-2735
Preprint. Discussion started: 7 December 2023

the last 50-years of the ensemble simulations. Nevertheless, to permit the most direct comparison where possible, we have matched our calculations to the periods used by other authors.

3.1 Continental trends in climate

Our simulated SAT trend over Antarctica is 0.12±0.02 °C per decade over the last 50 years (Figure 1). This is consistent with observations of 0.12±0.07 °C per decade over 1957-2006 (Steig et al., 2009) and 0.11±0.08 °C per decade over 1959-2012 (Nicolas and Bromwich, 2014). Our trend is lower than the 0.22±0.04 °C trend of Casado et al. (2023), however this is itself dependent on their isotope-to-temperature reconstruction method. Over East Antarctica, our simulated Historical SAT trend is weaker (0.10±0.02 °C per decade; r=0.59) than over the West Antarctica (0.15±0.02 °C per decade; r=0.75). This compares with 0.10±0.07 °C per decade for the East and 0.17±0.06 °C per decade for the West calculated by Steig et al. (2009).

Our simulated Historical precipitation trend over the last 50 years is 3.1 mm/y per decade (Figure 1), which lies between the, admittedly wide, Bromwich et al. (2011) reanalyses based equivalent values of 0.4±1.8 mm/y per decade from the Climate Forecast System Reanalysis (CFSR), and 7.1±1.5 mm/y per decade from the National Centers for Environmental Prediction reanalyses 2 (NCEP-2) over 1979-2009. The HadCM3 results are also is agreement with Dalaiden et al. (2020) who show an increase in both WAIS and EAIS simulated precipitation.

Our HadCM3 simulated Historical Antarctic September sea ice decrease is -0.20±0.01 x 10^6 km^2/decade over the period 1851-2004 (r=-0.69), and -0.40±0.06 x 10^6 km^2/decade over the period 1954–2004 (r=0.67). This is consistent with the recent results of Shu et al. (2020), who calculated Antarctic September sea ice trends of -0.45 and -0.43 x 10^6 km^2/decade during the period 1979–2005 from the Coupled Model Intercomparison Project (CMIP) 5 and 6 model results, respectively. Whilst neither the Shu et al. (2020) nor our HadCM3 sea ice trends match the observed slope of +0.10 x 10^6 km^2/decade (p=0.16) (Shu et al., 2020), they do agree with each other. It is also worth noting that, since 2016, Antarctic sea ice has begun losing significant area during both summer and winter.

The simulated Historical changes in Antarctic-wide SAT and precipitation and sea ice thus seem in reasonable agreement with other model results, and possibly also observations (though this is less clear). Trends, however, vary between regions.

3.2 Regional-scale trends

We now look at the simulated climate, using the Antarctic regions defined by the PAGES A2k community (see Figure 2, regions defined by Stenni et al., 2017).

3.2.1 SAT, precipitation, sea ice

Every Antarctic region shows a simulated increase in SAT over the Historical period (1851–2004, Figure 2, Table A1), but these vary across the continent. Warming trends are strongest for the Peninsula and Dronning Maud Land regions (0.11 °C per decade, and r≥0.8), closely followed by the WAIS and the Weddell coast regions (0.08 °C per decade, and r≥0.8). The

https://doi.org/10.5194/egusphere-2023-2735
Preprint. Discussion started: 7 December 2023

Plateau and the Indian coast show weaker warming trends of 0.04 and 0.05 °C per decade, respectively (r=0.6 for both). These historical trends approximately match Turner et al. (2020) results derived from station data.

Our simulated SAT trends resemble the Stenni et al. (2017) regional warming trends (Table A1). Stenni et al. (2017) found cooling trends for the Plateau, the Weddell coast, and Victoria Land (from -0.13 to -0.05 °C per decade), where we found a small warming; they found a larger trend for the Peninsula (from 0.2 to 0.29 °C per decade), though again we point out that the Stenni et al. (2017) values, like the Casado et al. (2023) results, are partly dependent on isotope-to-temperature reconstruction methods.

Similar to SAT, HadCM3 shows an increase in precipitation for all the Antarctic regions, both for the full Historical period, and for the last 50 years. Similar to temperature, the Peninsula features the strongest trend of 7.8 mm/y per decade over the Historical period, whereas the Plateau and the Ross sections display weaker trends of 0.5 and 0.82 mm/y per decade over the same period. Interestingly, Thomas et al. (2017) and (Medley and Thomas, 2019) found similar results. Whilst these results are from ice cores, these are not dependent on the interpretation of isotopes, instead they mostly use profiles of density and layer counting from relevant age markers (e.g. chemical species, radio isotopes, biologically compounds).

For sea ice, HadCM3 simulates a sea ice decrease around all sectors of Antarctica, except for Weddell sector (Table B1). Trends are largest in the Indian sector (-49±5 x 10^3 km^2 per decade; r=-0.67) and smallest for the Pacific sector (-25±4 x 10^3 km^2 per decade r=-0.44). Whilst these results are not compatible with pre-2016 satellite observations, they are consistent with other climate simulations (Shu et al., 2020).

3.2.2 $\delta^{18}O$

Despite the simulated increases in SAT and precipitation, $\delta^{18}O$ shows a very weak trend of 0.04±0.003 ‰ per decade (r=0.21) over the last 50 years. Interestingly, (Casado et al., 2023) provide a higher trend from 1950–2005 of 0.11±0.02 ‰ per decade. It is unclear why the trend in (Casado et al., 2023) is higher. Section 5 of this paper focuses on investigating and explaining the $\delta^{18}O$ trends. Before this, we provide a brief overview of the regional picture.

At the regional scale, over the Historical period, trends are small (Figure 2). It is null for the Victoria Land, and is the highest for the Weddell coast with a trend of 0.05 ‰ per decade (r=0.39), and the strongest for the peninsula with a trend of 0.04 ‰ per decade (r=0.57). Over the last fifty years, a part from the Victoria Land where a very weak trend appear, other regions present weaker trends with correlation coefficients now ranging from 0.11 to 0.38 while gradients increase with values ranging from 0.03 ‰ per decade for the WAIS and the plateau, to 0.14 ‰ per decade for the Weddell coast. Stenni et al. (2017) made a $\delta^{18}O$ trend statistics based on ice core anomalies using unweighted composites over the period 1900-2000. They found only 3 regions with significant trends, which are the Indian coast, the peninsula and Dronning Maud land, with gradients in the range of our results, while higher for the peninsula and Dronning Maud land (mean trends of 0.15 ‰ per decade and 0.11 ‰ per decade respectively). Comparatively, Casado et al. (2023) calculated trends over windows varying between 35 and 60 years and using a persistence method. They found values gradients with the same range of values, from 0.09 ‰ for the Indian coast, to 0.19 ‰ for the Weddell coast, while generally larger than those found in HadCM3 using the last fifty years, especially for the WAIS (0.03 ‰ per decade and 0.14 ‰ per decade, in our HadCM3 outputs and in Casado et al. (2023) respectively), Victoria

https://doi.org/10.5194/egusphere-2023-2735
Preprint. Discussion started: 7 December 2023

Land (0.04 ‰ per decade and 0.15 ‰ per decade, in our HadCM3 outputs and in Casado et al. (2023) respectively), and the plateau (0.03 ‰ per decade and 0.18 ‰ per decade, in our HadCM3 outputs and in Casado et al. (2023) respectively). These disparities could be explained by the different time windows, the different methodologies or the lack of ice core data to make representative regional reconstructions.

4 Temperature versus δ^{18}O relationships

Given that much of ice core science is underpinned by the relationship between temperature and δ^{18}O (Jouzel et al., 2003), and having discussed simulated SAT, precipitation, sea ice and δ^{18}O trends, we now investigate temperature versus δ^{18}O relationships. Sime et al. (2008) demonstrate that there is no clear relationship between the spatial versus temporal SAT-δ^{18}O gradients across Antarctica. We therefore focus on comparing the last 50 years of our simulations against the whole Historical period. To enable a consideration of model dependency, we also compare our Historical ensemble against a nudged ECHAM5 simulation (1979-2013), used in Stenni et al. (2017) (Table 1).

4.1 Antarctic-wide and regional scale

The simulated SAT-δ^{18}O relationship, calculated using annual means on each grid point, is statistically significant over 66% of Antarctica (Figure 3). For the continent as a whole, we simulate a mean Antarctic SAT-δ^{18}O gradient of 0.57±0.06 ‰/°C (r=0.62) over the Historical period, increasing to 0.67±0.13 (r=0.60) over the last 50 years of the simulation. The comparable numbers for an Antarctic-wide SAT-δ^{18}O relationship in Casado et al. (2023) are 0.49 to 0.69 ‰/°C. In our simulations, non significant SAT-δ^{18}O relationships occur in: the eastern parts of Antarctica between 40 and 100° E; all regions between 140 and 220° E covering the Wilkes coast, Victoria Land and some parts of Queen Mary Land; and the coast of Dronning Maud Land with some areas at 350-360° E joining the South Pole. Casado et al. (2023) also found no significant relationships, though possibly because of a lack of data, for some regions. For them, these regions were the Indian and Weddell coasts and Victoria Land. (Please see section 5 for a discussion of why these regions do not show statistically significant temperature versus δ^{18}O relationships). In contrast, the Peninsula, part of the WAIS coast, as well as some parts of the Plateau show much stronger SAT-δ^{18}O relationships. Indeed, some coastal areas are associated with the highest correlation coefficients, ranging between 0.15 and 0.45. The highest SAT-δ^{18}O gradients in the Plateau region, as well as south of the Filchner ice shelf, can exceed 0.75 ‰/°C. Casado et al. (2023) also found the largest SAT-δ^{18}O gradients in similar regions.

This Antarctic-wide picture of geographical variability in the temperature versus δ^{18}O relationship is reasonably consistent with previous studies covering parts of the Historical period (Sime et al., 2009a; Stenni et al., 2017; Goursaud et al., 2019), as well as measurements from coastal firn cores (Isaksson and Karlén, 1994; Abram et al., 2013; Thomas et al., 2013; Goursaud et al., 2017). Interestingly, Guan et al. (2016, 2020) associate similar results (low or negative SAT-δ^{18}O relationships) with higher source temperatures. Here, and also for other warm climate results (e.g. Sime et al., 2008, 2009b; Holloway et al., 2016, 2018), we suggest this is mainly driven by sea ice retreat (See section 5).

https://doi.org/10.5194/egusphere-2023-2735
Preprint. Discussion started: 7 December 2023

4.2 Stability over the Historical period and model dependency

Results from HadCM3 are similar for both the last 50 years and the whole Historical period (Table 1): SAT-δ^{18}O gradients vary between 0.3 to 0.7 ‰/°C. The average difference is 0.07 ‰/°C. The only region with a statistically different result is Dronning Maud Land, with SAT–δ^{18}O gradients of 0.76±0.12 ‰/°C and 0.49±0.05 ‰/°C over the last 50 years and the whole Historical period, respectively. Thus, for most of the continent, our HadCM3 results over the last 50 years and the whole Historical period appear equivalent.

Interestingly, however, this is not the case when comparing between the last 50 years of our HadCM3 simulation and the ECHAM5-wiso simulation. Both simulations show the same main features: excluding Victoria Land, gradients are the highest for the Plateau, the Weddell coast, the WAIS and DML regions (averaged gradients of 0.98±0.05 and 0.64±0.09 ‰/°C in ECHAM5-wiso and HadCM3, respectively), and the lowest for the Peninsula (0.40±0.02 and 0.28±0.05 ‰/°C in ECHAM5-wiso and HadCM3, respectively) regions. However, the ECHAM5-wiso gradients average 0.4 ‰/°C higher than those simulated by HadCM3. In addition to this consistent offset between the nudged ECHAM5-wiso and unnudged HadCM3 simulations, all the historical SAT-δ^{18}O relationships are different from the LGM-PI ECHAM5, and LIG-PI HadCM3 relationships: Werner et al. (2018) report LGM-PI regional gradients in ECHAM5 that are 17-26% lower, while (Sime et al., 2009b) and (Holloway et al., 2016) present LIG-PI regional gradients that are ∼50% lower for HadCM3. Thus, whilst it is unclear whether the nudging of ECHAM5 towards ERA-40 reanalysis, or differences in sea ice behaviours, are the main reason for these discrepancies, it is clear that simulated temperature versus δ^{18}O relationships have significant uncertainties. These need to be considered, both regionally and for the most relevant climate state, before being undertaking any inferences of past temperatures using isotopes measured in ice cores.

5 Drivers of δ^{18}O changes

We use two approaches to investigate the mechanisms driving simulated δ^{18}O changes. First, we separate and compare extreme warm and cold years (Figure 4, Table C1) by generating composites with mean annual Antarctic SAT anomalies greater than plus or minus two standard deviations from the mean, respectively. Second, we isolate the impact of changing precipitation seasonality on δ^{18}O, following the method used in Liu and Battisti (2015); Holloway et al. (2016) and Sime et al. (2019).

As expected, the spatial patterns of SAT, and sea ice anomalies are strongly correlated, and the pattern is approximately mirrored between cold and warm composites (Figure 4, top and bottom panels, respectively). The primary mechanism driving continental-scale SAT-δ^{18}O decoupling is the simulated loss of sea ice during the historical period (Figure 5DH). The September average sea ice area across the warm composite is 5.8 x10^6 km^2 less than in the cold composite. Given that this reduction occurs primarily during winter (Figure 5c; there is almost no summertime sea ice around Antarctica), warmer years tend to receive relatively more precipitation during winter months compared to cold years, partially offsetting the warming signal in δ^{18}O. This can be seen in Figure 5, displaying seasonal anomalies in precipitation, δ^{18}O and sea ice between the warm and cold composites: The largest (smallest) precipitation and δ^{18}O anomalies occur during winter (summer) months. Precipitation anomalies peak in autumn and winter, whilst δ^{18}O anomalies peak in winter and spring (Figure 6), the latter coincident with the

https://doi.org/10.5194/egusphere-2023-2735
Preprint. Discussion started: 7 December 2023

annual maximum sea ice extent and largest sea ice area anomalies. The relative increase in winter precipitation during warm years acts to reduce δ^{18}O across Antarctica, compared to if the seasonality of precipitation remained unchanged. Spatially, the effect of changing seasonality is largest in the Indian, Dronning Maud Land and Victoria Land (through the Wilkes Land) sectors (Figure 5c).

Although the reduction in sea ice area simulated in the warm composite and throughout the Historical ensemble increases the proportion of winter precipitation, negatively influencing δ^{18}O, less sea ice also shortens the distance between evaporation source and precipitation site, which has an opposing positive influence on δ^{18}O. This effect is evident as negative sea ice anomalies adjacent to coastal regions with large positive δ^{18}O anomalies in Figure 7b as well as in Figures 5eh. Sea ice loss may also allow locally sourced precipitation to penetrate further inland into the Antarctic interior, which usually receives precipitation sourced from lower latitudes (Gao et al., 2023), as well as promoting an increase in high intensity precipitation events during cold seasons (e.g. Schlosser et al., 2004). Consequently, sea ice loss during the Historical period leads to competing influences on δ^{18}O and considerable spatial variability in SAT-δ^{18}O relationships (Figure 3a), with no significant relationship in several regions. Changes in the precipitation seasonality (Figure 7a) reduce mean Antarctic $\delta^{18}O$ by 0.16$\pm$0.19 ‰ and for the lowest changes by 0.11 ‰ over the Plateau and no changes over the Peninsula. Changes in the seasonal cycle of δ^{18}O (Figure 7b) are more spatially variable and largely sea-ice driven, with a depletion up to -0.45 ‰ over the Plateau and Victoria Land and an enrichment from 0.1 to 1.0 ‰ in coastal regions.

These Historical simulations indicate that Antarctic δ^{18}O is highly sensitive to patterns of sea ice change, which influence atmospheric dynamics, air mass pathways and lengths, and water isotope evaporation and condensation temperatures. Our results are particularly sensitive to autumnal sea ice changes: the largest simulated reduction in sea ice occurs in Autumn, coincident with the largest changes in δ^{18}O (Figure 5c).

6 Conclusions

Results from six transient simulations over the Historical period allow us to examine Antarctic precipitation weighted δ^{18}O and its relationship with Antarctic SAT. The ensemble features a rise of mean-Antarctic SAT of 0.12$\pm$0.02 °C/decade over the last 50 years, consistent with previous studies Steig et al. (2009); Nicolas and Bromwich (2014). In agreement with observations, the associated simulated trend in the water isotope δ^{18}O is weak (+0.04$\pm$0.03 ‰/decade). Unlike SAT, the δ^{18}O trend is weaker during the last 50 years, compared to the complete Historical period. This implies that over the last fifty years of our ensemble, δ^{18}O is influenced by processes other than SAT-related condensation temperature, *i.e.* ice and atmospheric processes oppose purely SAT and condensation temperature controls on δ^{18}O.

Although the consequences of these competing effects vary spatially, they result in non-statistically significant relationships between SAT and δ^{18}O for approximately one third of the continent over the Historical ensemble. Non-significant SAT-δ^{18}O relationships occur across much of Antarctica between 40 and 100° E; the Wilkes coast, Victoria Land, part of Queen Mary Land; the coast of Dronning Maud Land, and areas of the South Pole region. Interestingly, we find lower SAT-δ^{18}O correlations and gradients compared to ERA5-nudged ECHAM5-wiso simulations, both at the regional and individual ice core scale.

https://doi.org/10.5194/egusphere-2023-2735
Preprint. Discussion started: 7 December 2023

We identify three processes that lead to weak SAT-δ^{18}O relationships during the Historical ensemble. Firstly, Historical changes in near-coastal air mass intrusions, induced by changes in the large-scale circulation and/or changes in synoptic events, have an impact on both the moisture source and precipitation regime. Secondly, changes in sea ice concentration impact moisture pathways to Antarctica. And thirdly, changes in precipitation seasonality, largely driven by sea ice changes, biases the relative impact of cold vs warm season precipitation on precipitation-weighted δ^{18}O. Fyke et al. (2017) show similar spatial patterns in Antarctic precipitation during the pre-industrial (Fyke et al. (2017), Fig 2.c), driven by the large-scale circulation and acting to regulate atmospheric moisture transport and regional sea ice variability (Fyke et al., 2017; Marshall et al., 2017; Raphael et al., 2019). Changes in Antarctic sea ice (Holloway et al., 2016) and moisture source changes (Landais et al., 2021) have also been proposed as responsible for driving the Last Interglacial δ^{18}O peak. Additionally, Sime et al. (2008) show that (sea ice related) changes in the seasonal and synoptic distribution of Antarctic precipitation were jointly responsible for a partial decoupling between SAT and δ^{18}O. These results support the role of environmental changes, particularly sea ice, generating significant variability in the Antarctic SAT–δ^{18}O relationship.

In conclusion, the results from this isotope-enabled Historical ensemble permit investigation of the SAT–δ^{18}O relationship during the Historical period and the mechanisms driving its spatial variability. Whilst we recognise the limitations, in terms of spatial resolution and a simplistic sea ice sub-model, of our chosen model, HadCM3, we value the ability to perform a several-member ensemble of $>$100-year simulations using a fully coupled, isotope-enabled model.

For future work, Higher resolution and more physically advanced models could be used, alongside new tracer methods (Gao et al., 2023). Firn model could also be used to examine the interesting question of post-deposition effects such as the redistribution of snow by the wind (Libois et al., 2014), snow-vapour exchanges (Casado et al., 2016; Ritter et al., 2016), and snow metamorphism (Casado et al., 2021) on Historical δ^{18}O. Finally, more water stable isotope records from Antarctic ice and firn core data are more than needed to evaluate models, as well as to lead model-data investigations of past climates.

Code and data availability. The code and the simulation outputs can be made available on request.

Author contributions. SGO and LCS co-designed the study. MH ran all simulations. SGO conducted all analysis and produced all figures. SGO and LCS co-wrote the first draft of the manuscript. All authors contributed to the final manuscript version.

Competing interests. The authors declare that they have no conflict of interest.

Acknowledgements. This work has received support from the NERC National Capability International grant SURface FluxEs In AnTarctica (SURFEIT): NE/X009319/1. LCS acknowledges additional support from DEEPICE: Understanding Deep Ice Core Proxies to Infer Past

https://doi.org/10.5194/egusphere-2023-2735
Preprint. Discussion started: 7 December 2023

Antarctic Climate Dynamics, EU-H2020 G.N.955750; ANTSIE: ANTarctic Sea Ice Evolution from a novel biological archive: EU-H2020 G.N.864637 and TiPES: Tipping Points in the Earths System: EU-H2020 G.N.820970. Simulations were run and analysed on NERC's ARCHER2 and JASMIN platforms.

https://doi.org/10.5194/egusphere-2023-2735
Preprint. Discussion started: 7 December 2023

References

Consistent multidecadal variability in global temperature reconstructions and simulations over the Common Era, Nature geoscience, 12, 643–649, 2019.

Abram, N. J., Mulvaney, R., Wolff, E. W., Triest, J., Kipfstuhl, S., Trusel, L. D., Vimeux, F., Fleet, L., and Arrowsmith, C.: Acceleration of snow melt in an Antarctic Peninsula ice core during the twentieth century, Nature Geoscience, 6, 404–411, 2013.

Andrews, M. B., Ridley, J. K., Wood, R. A., Andrews, T., Blockley, E. W., Booth, B., Burke, E., Dittus, A. J., Florek, P., Gray, L. J., et al.: Historical simulations with HadGEM3-GC3. 1 for CMIP6, Journal of Advances in Modeling Earth Systems, 12, e2019MS001 995, 2020.

Bromwich, D. H., Nicolas, J. P., and Monaghan, A. J.: An assessment of precipitation changes over Antarctica and the Southern Ocean since 1989 in contemporary global reanalyses, Journal of Climate, 24, 4189–4209, 2011.

Casado, M., Landais, A., Masson-Delmotte, V., Genthon, C., Kerstel, E., Kassi, S., Arnaud, L., Picard, G., Prie, F., Cattani, O., et al.: Continuous measurements of isotopic composition of water vapour on the East Antarctic Plateau, Atmospheric Chemistry and Physics, 16, 8521–8538, 2016.

Casado, M., Landais, A., Picard, G., Arnaud, L., Dreossi, G., Stenni, B., and Prie, F.: Water isotopic signature of surface snow metamorphism in Antarctica, Geophysical Research Letters, 48, e2021GL093 382, 2021.

Casado, M., Hébert, R., Faranda, D., and Landais, A.: The quandary of detecting the signature of climate change in Antarctica, Nature Climate Change, pp. 1–7, 2023.

Dalaiden, Q., Goosse, H., Lenaerts, J. T., Cavitte, M. G., and Henderson, N.: Future Antarctic snow accumulation trend is dominated by atmospheric synoptic-scale events, Communications Earth & Environment, 1, 62, 2020.

Dansgaard, W.: The abundance of O18 in atmospheric water and water vapour, Tellus, 5, 461–469, 1953.

Edwards, T. L., Nowicki, S., Marzeion, B., Hock, R., Goelzer, H., Seroussi, H., Jourdain, N. C., Slater, D. A., Turner, F. E., Smith, C. J., et al.: Projected land ice contributions to twenty-first-century sea level rise, Nature, 593, 74–82, 2021.

Eyring, V., Bony, S., Meehl, G. A., Senior, C. A., Stevens, B., Stouffer, R. J., and Taylor, K. E.: Overview of the Coupled Model Intercomparison Project Phase 6 (CMIP6) experimental design and organization, Geoscientific Model Development, 9, 1937–1958, 2016.

Fyke, J., Lenaerts, J., and Wang, H.: Basin-scale heterogeneity in Antarctic precipitation and its impact on surface mass variability, The Cryosphere, 11, 2595–2609, 2017.

Gao, M., Kim, S.-J., Yang, J., Liu, J., Jiang, T., Su, B., Wang, Y., and Huang, J.: Historical fidelity and future change of Amundsen Sea Low under 1.5° C–4° C global warming in CMIP6, Atmospheric Research, 255, 105 533, 2021.

Gao, Q., Sime, L., McLaren, A., Bracegirdle, T. J., Capron, E., Rhodes, R. H., Steen-Larsen, H. C., Shi, X., and Werner, M.: Evaporative controls on Antarctic precipitation: An ECHAM6 model study using novel water tracer diagnostics, EGUsphere, 2023, 1–38, 2023.

Garbe, J., Albrecht, T., Levermann, A., Donges, J. F., and Winkelmann, R.: The hysteresis of the Antarctic ice sheet, Nature, 585, 538–544, 2020.

Golledge, N. R., Keller, E. D., Gomez, N., Naughten, K. A., Bernales, J., Trusel, L. D., and Edwards, T. L.: Global environmental consequences of twenty-first-century ice-sheet melt, Nature, 566, 65–72, 2019.

Goosse, H., Braida, M., Crosta, X., Mairesse, A., Masson-Delmotte, V., Mathiot, P., Neukom, R., Oerter, H., Philippon, G., Renssen, H., et al.: Antarctic temperature changes during the last millennium: evaluation of simulations and reconstructions, Quaternary Science Reviews, 55, 75–90, 2012.

https://doi.org/10.5194/egusphere-2023-2735
Preprint. Discussion started: 7 December 2023

Gordon, C., Cooper, C., Senior, C. A., Banks, H., Gregory, J. M., Johns, T. C., Mitchell, J. F., and Wood, R. A.: The simulation of SST, sea ice extents and ocean heat transports in a version of the Hadley Centre coupled model without flux adjustments, Climate dynamics, 16, 147–168, 2000.

Goursaud, S., Masson-Delmotte, V., Favier, V., Preunkert, S., Fily, M., Gallée, H., Jourdain, B., Legrand, M., Magand, O., Minster, B., et al.: A 60-year ice-core record of regional climate from Adélie Land, coastal Antarctica, The Cryosphere, 11, 343–362, 2017.

Goursaud, S., Masson-Delmotte, V., Favier, V., Orsi, A., and Werner, M.: Water stable isotope spatio-temporal variability in Antarctica in 1960–2013: observations and simulations from the ECHAM5-wiso atmospheric general circulation model, Climate of the Past, 14, 923–946, 2018.

Goursaud, S., Masson-Delmotte, V., Favier, V., Preunkert, S., Legrand, M., Minster, B., and Werner, M.: Challenges associated with the climatic interpretation of water stable isotope records from a highly resolved firn core from Adélie Land, coastal Antarctica, The Cryosphere, 13, 1297–1324, 2019.

Goursaud, S., Holloway, M., Sime, L., Wolff, E., Valdes, P., Steig, E. J., and Pauling, A.: Antarctic Ice Sheet elevation impacts on water isotope records during the Last Interglacial, Geophysical Research Letters, 48, e2020GL091 412, 2021.

Graham, A. G., Wåhlin, A., Hogan, K. A., Nitsche, F. O., Heywood, K. J., Totten, R. L., Smith, J. A., Hillenbrand, C.-D., Simkins, L. M., Anderson, J. B., et al.: Rapid retreat of Thwaites Glacier in the pre-satellite era, Nature Geoscience, 15, 706–713, 2022.

Guan, J., Liu, Z., Wen, X., Brady, E., Noone, D., Zhu, J., and Han, J.: Understanding the temporal slope of the temperature-water isotope relation during the deglaciation using isoCAM3: The slope equation, Journal of Geophysical Research: Atmospheres, 121, 10–342, 2016.

Guan, J., Liu, Z., and Chen, G.: Moisture Source Tagging Confirming the Polar Amplification Effect in Amplifying the Temperature-δ18O Temporal Slope Since the LGM, Atmosphere, 11, 610, 2020.

Holloway, M. D., Sime, L., Singarayer, J. S., Tindall, J. C., Bunch, P., and Valdes, P. J.: Antarctic last interglacial isotope peak in response to sea ice retreat not ice-sheet collapse, Nature communications, 7, 1–9, 2016.

Holloway, M. D., Sime, L., Singarayer, J. S., Tindall, J. C., and Valdes, P. J.: Simulating the 128-ka Antarctic Climate Response to Northern Hemisphere Ice Sheet Melting Using the Isotope-Enabled HadCM3, Geophysical Research Letters, 45, 11–921, 2018.

Isaksson, E. and Karlén, W.: Spatial and temporal patterns in snow accumulation, western Dronning Maud Land, Antarctica, Journal of Glaciology, 40, 399–409, 1994.

Johns, T., Gregory, J., Ingram, W., Johnson, C., Jones, A., Lowe, J., Mitchell, J., Roberts, D., Sexton, D., Stevenson, D., et al.: Anthropogenic climate change for 1860 to 2100 simulated with the HadCM3 model under updated emissions scenarios, Climate dynamics, 20, 583–612, 2003.

Jouzel, J., Vimeux, F., Caillon, N., Delaygue, G., Hoffmann, G., Masson-Delmotte, V., and Parrenin, F.: Magnitude of isotope/temperature scaling for interpretation of central Antarctic ice cores, Journal of Geophysical Research: Atmospheres, 108, 2003.

Jouzel, J., Masson-Delmotte, V., Cattani, O., Dreyfus, G., Falourd, S., Hoffmann, G., Minster, B., Nouet, J., Barnola, J.-M., Chappellaz, J., et al.: Orbital and millennial Antarctic climate variability over the past 800,000 years, science, 317, 793–796, 2007.

Krinner, G. and Werner, M.: Impact of precipitation seasonality changes on isotopic signals in polar ice cores: a multi-model analysis, Earth and Planetary Science Letters, 216, 525–538, 2003.

Lambert, F., Delmonte, B., Petit, J.-R., Bigler, M., Kaufmann, P. R., Hutterli, M. A., Stocker, T. F., Ruth, U., Steffensen, J. P., and Maggi, V.: Dust-climate couplings over the past 800,000 years from the EPICA Dome C ice core, Nature, 452, 616–619, 2008.

Landais, A., Casado, M., Prie, F., Magand, O., Arnaud, L., Ekaykin, A., Petit, J.-R., Picard, G., Fily, M., Minster, B., et al.: Surface studies of water isotopes in Antarctica for quantitative interpretation of deep ice core data, Comptes Rendus Geoscience, 349, 139–150, 2017.

https://doi.org/10.5194/egusphere-2023-2735
Preprint. Discussion started: 7 December 2023

Landais, A., Stenni, B., Masson-Delmotte, V., Jouzel, J., Cauquoin, A., Fourré, E., Minster, B., Selmo, E., Extier, T., Werner, M., et al.: Interglacial Antarctic–Southern Ocean climate decoupling due to moisture source area shifts, Nature Geoscience, 14, 918–923, 2021.

Libois, Q., Picard, G., Arnaud, L., Morin, S., and Brun, E.: Modeling the impact of snow drift on the decameter-scale variability of snow properties on the Antarctic Plateau, Journal of Geophysical Research: Atmospheres, 119, 11–662, 2014.

Liu, X. and Battisti, D. S.: The influence of orbital forcing of tropical insolation on the climate and isotopic composition of precipitation in South America, Journal of Climate, 28, 4841–4862, 2015.

Lorius, C. and Merlivat, L.: Distribution of mean surface stable isotope values in East Antarctica, Isotopes and Impurities in Snow and Ice, IAHS, Pub, 118, 127–137, 1977.

Marshall, G. J., Thompson, D. W., and van den Broeke, M. R.: The signature of Southern Hemisphere atmospheric circulation patterns in Antarctic precipitation, Geophysical Research Letters, 44, 11–580, 2017.

Masson, V., Vimeux, F., Jouzel, J., Morgan, V., Delmotte, M., Ciais, P., Hammer, C., Johnsen, S., Lipenkov, V. Y., Mosley-Thompson, E., et al.: Holocene climate variability in Antarctica based on 11 ice-core isotopic records, Quaternary Research, 54, 348–358, 2000.

Masson-Delmotte, V., Hou, S., Ekaykin, A., Jouzel, J., Aristarain, A., Bernardo, R., Bromwich, D., Cattani, O., Delmotte, M., Falourd, S., et al.: A review of Antarctic surface snow isotopic composition: Observations, atmospheric circulation, and isotopic modeling, Journal of climate, 21, 3359–3387, 2008.

Masson-Delmotte, V., Stenni, B., Pol, K., Braconnot, P., Cattani, O., Falourd, S., Kageyama, M., Jouzel, J., Landais, A., Minster, B., et al.: EPICA Dome C record of glacial and interglacial intensities, Quaternary Science Reviews, 29, 113–128, 2010.

Medley, B. and Thomas, E.: Increased snowfall over the Antarctic Ice Sheet mitigated twentieth-century sea-level rise, Nature Climate Change, 9, 34–39, 2019.

Milillo, P., Rignot, E., Rizzoli, P., Scheuchl, B., Mouginot, J., Bueso-Bello, J. L., Prats-Iraola, P., and Dini, L.: Rapid glacier retreat rates observed in West Antarctica, Nature Geoscience, 15, 48–53, 2022.

Miller, R. L., Schmidt, G. A., Nazarenko, L. S., Bauer, S. E., Kelley, M., Ruedy, R., Russell, G. L., Ackerman, A. S., Aleinov, I., Bauer, M., et al.: CMIP6 Historical Simulations (1850–2014) With GISS-E2. 1, Journal of Advances in Modeling Earth Systems, 13, e2019MS002 034, 2021.

Neukom, R., Schurer, A. P., Steiger, N., Hegerl, G. C., et al.: Possible causes of data model discrepancy in the temperature history of the last Millennium, Scientific Reports, 8, 1–15, 2018.

Nicolas, J. P. and Bromwich, D. H.: New reconstruction of Antarctic near-surface temperatures: Multidecadal trends and reliability of global reanalyses, Journal of Climate, 27, 8070–8093, 2014.

Parsons, L. A., Brennan, M. K., Wills, R. C., and Proistosescu, C.: Magnitudes and spatial patterns of interdecadal temperature variability in CMIP6, Geophysical Research Letters, 47, e2019GL086 588, 2020.

Pohl, B., Favier, V., Wille, J., Udy, D. G., Vance, T. R., Pergaud, J., Dutrievoz, N., Blanchet, J., Kittel, C., Amory, C., et al.: Relationship between weather regimes and atmospheric rivers in East Antarctica, Journal of Geophysical Research: Atmospheres, 126, e2021JD035 294, 2021.

Pope, V., Gallani, M., Rowntree, P., and Stratton, R.: The impact of new physical parametrizations in the Hadley Centre climate model: HadAM3, Climate dynamics, 16, 123–146, 2000.

Pörtner, H.-O., Roberts, D. C., Adams, H., Adler, C., Aldunce, P., Ali, E., Begum, R. A., Betts, R., Kerr, R. B., Biesbroek, R., et al.: Climate change 2022: Impacts, adaptation and vulnerability, IPCC Sixth Assessment Report, 2022.

https://doi.org/10.5194/egusphere-2023-2735
Preprint. Discussion started: 7 December 2023

Post, E., Alley, R. B., Christensen, T. R., Macias-Fauria, M., Forbes, B. C., Gooseff, M. N., Iler, A., Kerby, J. T., Laidre, K. L., Mann, M. E., et al.: The polar regions in a 2 C warmer world, Science advances, 5, eaaw9883, 2019.

Purich, A. and England, M. H.: Historical and Future Projected Warming of Antarctic Shelf Bottom Water in CMIP6 Models, Geophysical Research Letters, 48, e2021GL092 752, 2021.

Raphael, M. N. and Handcock, M. S.: A new record minimum for Antarctic sea ice, Nature Reviews Earth & Environment, 3, 215–216, 2022.

Raphael, M. N., Holland, M. M., Landrum, L., and Hobbs, W. R.: Links between the Amundsen Sea Low and sea ice in the Ross Sea: seasonal and interannual relationships, Climate Dynamics, 52, 2333–2349, 2019.

Raphael, M. N., Handcock, M. S., Holland, M. M., and Landrum, L. L.: An assessment of the temporal variability in the annual cycle of daily Antarctic sea ice in the NCAR Community Earth System Model, Version 2: A comparison of the historical runs with observations, Journal of Geophysical Research: Oceans, 125, e2020JC016 459, 2020.

Ritter, F., Steen-Larsen, H. C., Werner, M., Masson-Delmotte, V., Orsi, A., Behrens, M., Birnbaum, G., Freitag, J., Risi, C., and Kipfstuhl, S.: Isotopic exchange on the diurnal scale between near-surface snow and lower atmospheric water vapor at Kohnen station, East Antarctica, The Cryosphere, 10, 1647–1663, 2016.

Roach, L. A., Dörr, J., Holmes, C. R., Massonnet, F., Blockley, E. W., Notz, D., Rackow, T., Raphael, M. N., O'Farrell, S. P., Bailey, D. A., et al.: Antarctic sea ice area in CMIP6, Geophysical Research Letters, 47, e2019GL086 729, 2020.

Rong, X., Li, J., Chen, H., Su, J., Hua, L., Zhang, Z., and Xin, Y.: The CMIP6 historical simulation datasets produced by the climate system model CAMS-CSM, Advances in Atmospheric Sciences, 38, 285–295, 2021.

Schlosser, E., Reijmer, C., Oerter, H., and Graf, W.: The influence of precipitation origin on the δ18O–T relationship at Neumayer Station, Ekstrmisen, Antarctica, Annals of Glaciology, 39, 41–48, 2004.

Schurer, A. P., Tett, S. F., and Hegerl, G. C.: Small influence of solar variability on climate over the past millennium, Nature Geoscience, 7, 104–108, 2014.

Seroussi, H., Nowicki, S., Payne, A. J., Goelzer, H., Lipscomb, W. H., Abe-Ouchi, A., Agosta, C., Albrecht, T., Asay-Davis, X., Barthel, A., et al.: ISMIP6 Antarctica: a multi-model ensemble of the Antarctic ice sheet evolution over the 21st century, The Cryosphere, 14, 3033–3070, 2020.

Shu, Q., Wang, Q., Song, Z., Qiao, F., Zhao, J., Chu, M., and Li, X.: Assessment of sea ice extent in CMIP6 with comparison to observations and CMIP5, Geophysical Research Letters, 47, e2020GL087 965, 2020.

Sime, L., Tindall, J. C., Wolff, E. W., Connolley, W. M., and Valdes, P. J.: Antarctic isotopic thermometer during a CO2 forced warming event, Journal of Geophysical Research: Atmospheres, 113, 2008.

Sime, L., Marshall, G. J., Mulvaney, R., and Thomas, E. R.: Interpreting temperature information from ice cores along the Antarctic Peninsula: ERA40 analysis, Geophysical Research Letters, 36, 2009a.

Sime, L., Wolff, E., Oliver, K., and Tindall, J.: Evidence for warmer interglacials in East Antarctic ice cores, Nature, 462, 342–345, 2009b.

Sime, L., Hopcroft, P. O., and Rhodes, R. H.: Impact of abrupt sea ice loss on Greenland water isotopes during the last glacial period, Proceedings of the National Academy of Sciences, 116, 4099–4104, 2019.

Smerdon, J. E. et al.: Continental-scale temperature variability in PMIP3 simulations and PAGES 2k regional temperature reconstructions over the past millennium, 2015.

Steig, E. J., Schneider, D. P., Rutherford, S. D., Mann, M. E., Comiso, J. C., and Shindell, D. T.: Warming of the Antarctic ice-sheet surface since the 1957 International Geophysical Year, Nature, 457, 459–462, 2009.

https://doi.org/10.5194/egusphere-2023-2735
Preprint. Discussion started: 7 December 2023

Stenni, B., Curran, M. A., Abram, N. J., Orsi, A., Goursaud, S., Masson-Delmotte, V., Neukom, R., Goosse, H., Divine, D., Van Ommen, T., et al.: Antarctic climate variability on regional and continental scales over the last 2000 years, Climate of the Past, 13, 1609–1634, 2017.

Taylor, K. E., Stouffer, R. J., and Meehl, G. A.: An overview of CMIP5 and the experiment design, Bulletin of the American meteorological Society, 93, 485–498, 2012.

Thomas, E. R., Bracegirdle, T. J., Turner, J., and Wolff, E. W.: A 308 year record of climate variability in West Antarctica, Geophysical Research Letters, 40, 5492–5496, 2013.

Thomas, E. R., Van Wessem, J. M., Roberts, J., Isaksson, E., Schlosser, E., Fudge, T. J., Vallelonga, P., Medley, B., Lenaerts, J., Bertler, N., et al.: Regional Antarctic snow accumulation over the past 1000 years, Climate of the Past, 13, 1491–1513, 2017.

Tindall, J., Valdes, P., and Sime, L.: Stable water isotopes in HadCM3: Isotopic signature of El Niño–Southern Oscillation and the tropical amount effect, Journal of Geophysical Research: Atmospheres, 114, 2009.

Turner, J., Colwell, S. R., Marshall, G. J., Lachlan-Cope, T. A., Carleton, A. M., Jones, P. D., Lagun, V., Reid, P. A., and Iagovkina, S.: The SCAR READER project: Toward a high-quality database of mean Antarctic meteorological observations, Journal of Climate, 17, 2890–2898, 2004.

Turner, J., Connolley, W., Lachlan-Cope, T., and Marshall, G.: The performance of the Hadley Centre Climate Model (HadCM3) in high southern latitudes, International Journal of Climatology: A Journal of the Royal Meteorological Society, 26, 91–112, 2006.

Turner, J., Marshall, G. J., Clem, K., Colwell, S., Phillips, T., and Lu, H.: Antarctic temperature variability and change from station data, International Journal of Climatology, 40, 2986–3007, 2020.

Turner, J., Holmes, C., Caton Harrison, T., Phillips, T., Jena, B., Reeves-Francois, T., Fogt, R., Thomas, E. R., and Bajish, C.: Record low Antarctic sea ice cover in February 2022, Geophysical Research Letters, 49, e2022GL098 904, 2022.

van Ommen, T. D. and Morgan, V.: Calibrating the ice core paleothermometer using seasonality, Journal of Geophysical Research: Atmospheres, 102, 9351–9357, 1997.

Werner, M., Heimann, M., and Hoffmann, G.: Isotopic composition and origin of polar precipitation in present and glacial climate simulations, Tellus B: Chemical and Physical Meteorology, 53, 53–71, 2001.

Werner, M., Jouzel, J., Masson-Delmotte, V., and Lohmann, G.: Reconciling glacial Antarctic water stable isotopes with ice sheet topography and the isotopic paleothermometer, Nature communications, 9, 1–10, 2018.

Wille, J. D., Favier, V., Dufour, A., Gorodetskaya, I. V., Turner, J., Agosta, C., and Codron, F.: West Antarctic surface melt triggered by atmospheric rivers, Nature Geoscience, 12, 911–916, 2019.

Wille, J. D., Favier, V., Jourdain, N. C., Kittel, C., Turton, J. V., Agosta, C., Gorodetskaya, I. V., Picard, G., Codron, F., Santos, C. L.-D., et al.: Intense atmospheric rivers can weaken ice shelf stability at the Antarctic Peninsula, Communications Earth & Environment, 3, 90, 2022.

Wolff, E., Barbante, C., Becagli, S., Bigler, M., Boutron, C., Castellano, E., De Angelis, M., Federer, U., Fischer, H., Fundel, F., et al.: Changes in environment over the last 800,000 years from chemical analysis of the EPICA Dome C ice core, Quaternary Science Reviews, 29, 285–295, 2010.

Yoshimura, K., Kanamitsu, M., Noone, D., and Oki, T.: Historical isotope simulation using reanalysis atmospheric data, Journal of Geophysical Research: Atmospheres, 113, 2008.

https://doi.org/10.5194/egusphere-2023-2735
Preprint. Discussion started: 7 December 2023

Table

Table 1. Historical SAT–δ^{18}O relationships at the regional scale. Slope (in ‰/°C) plus or minus the standard error, and the correlation coefficient (into brackets) of the surface-weighed average of surface air temperature against the surface-weighed average of δ^{18}O for the Antarctic regions as defined in the PAGES Antarctica2k project (Stenni et al., 2017): the plateau, the Indian coast, the Weddell coast, the Peninsula, the WAIS, Victoria Land and Dronning Maud Land, simulated by the ECHAM5-wiso model (Stenni et al., 2017, over the period 1979-2013, 35 points, 'ECHAM5-wiso'), and simulated by HadCM3 over he last 50 years (1955-2004, 50 points, 'last 50 years of HadCM3'), and over the whole historical simulated period (1851-2004, 154 points, 'Historical HadCM3') using the ensemble mean of the six simulations (see methods). All the relationships are significant (p-values<0.05).

	ECHAM5-wiso	**last 50 years of HadCM3**	**Historical HadCM3**
Plateau	1.05±0.06 [0.62]	0.61±0.14 [0.52]	0.57±0.07 [0.53]
Indian coast	0.52±0.03 [0.44]	0.55±0.15 [0.46]	0.67±0.07 [0.59]
Weddell coast	0.99±0.06 [0.34]	0.57±0.11 [0.59]	0.57±0.07 [0.57]
Peninsula	0.40±0.02 [0.31]	0.28±0.06 [0.52]	0.31±0.02 [0.71]
WAIS	0.96±0.05 [0.59]	0.60±0.12 [0.58]	0.50±0.05 [0.61]
Victoria Land	1.21±0.07 [0.49]	-	0.30±0.12 [0.19]
Dronning Maud Land	0.93±0.05 [0.39]	0.76±0.12 [0.69]	0.49±0.05 [0.60]
West Antarctica	0.97±0.05 [0.62]	0.50±0.10 [0.57]	0.70±0.07 [0.62]
East Antarctica	1.00±0.05 [0.58]	0.49±0.10 [0.57]	0.56±0.06 [0.58]
All Antarctica	0.98±0.05 [0.56]	0.67±0.13 [0.60]	0.57±0.06 [0.62]

https://doi.org/10.5194/egusphere-2023-2735
Preprint. Discussion started: 7 December 2023

Figures

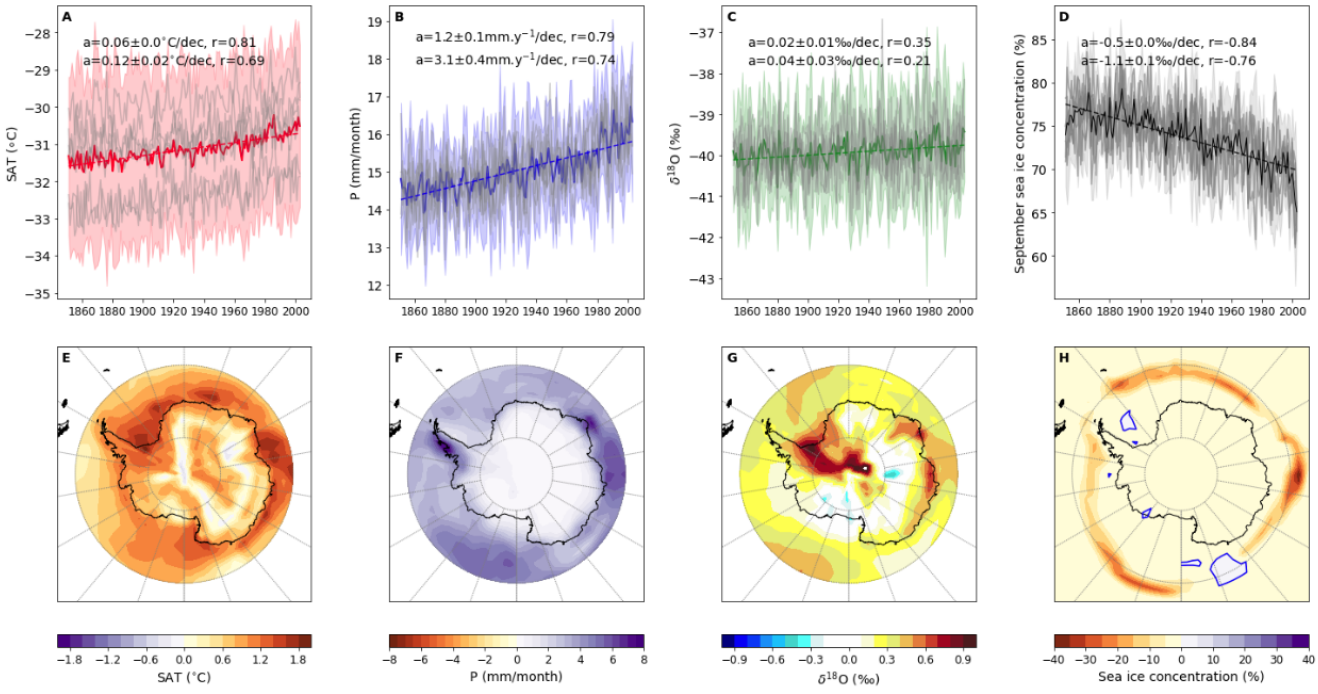

Figure 1. Antarctic trends over the periods 1851-2004 and 1955-2004. Each column is associated to a climate variable: the first column for the (**A, E**) surface air temperature ("SAT" in °C, in red), the second column for the (**B, F**) precipitation ("P in mm/month", in blue), (**C, G**) $\delta^{18}O$ (in ‰, in green) and (**D, H**) sea-ice concentration ("SIC" in %, in grey). The first row displays the time series of Antarctic surface weighted averages over the period 1851–2004. Colored solid lines represent the annual average of the ensemble mean, the colored surfaces represent the annual standard deviations of the ensemble mean, the grey solid lines the simulations, and the dashed lines, the linear regressions. The slopes ("a") plus or minus the standard errors, as well as the correlation coefficients ("r") are given on the top right of the figures, with the first value calculated over the whole historical period 1851–2004, and the second value over the last 50 years 1955–2004. The second row displays the map of anomalies over the periods 1955–2004 against 1854–1904.

https://doi.org/10.5194/egusphere-2023-2735
Preprint. Discussion started: 7 December 2023

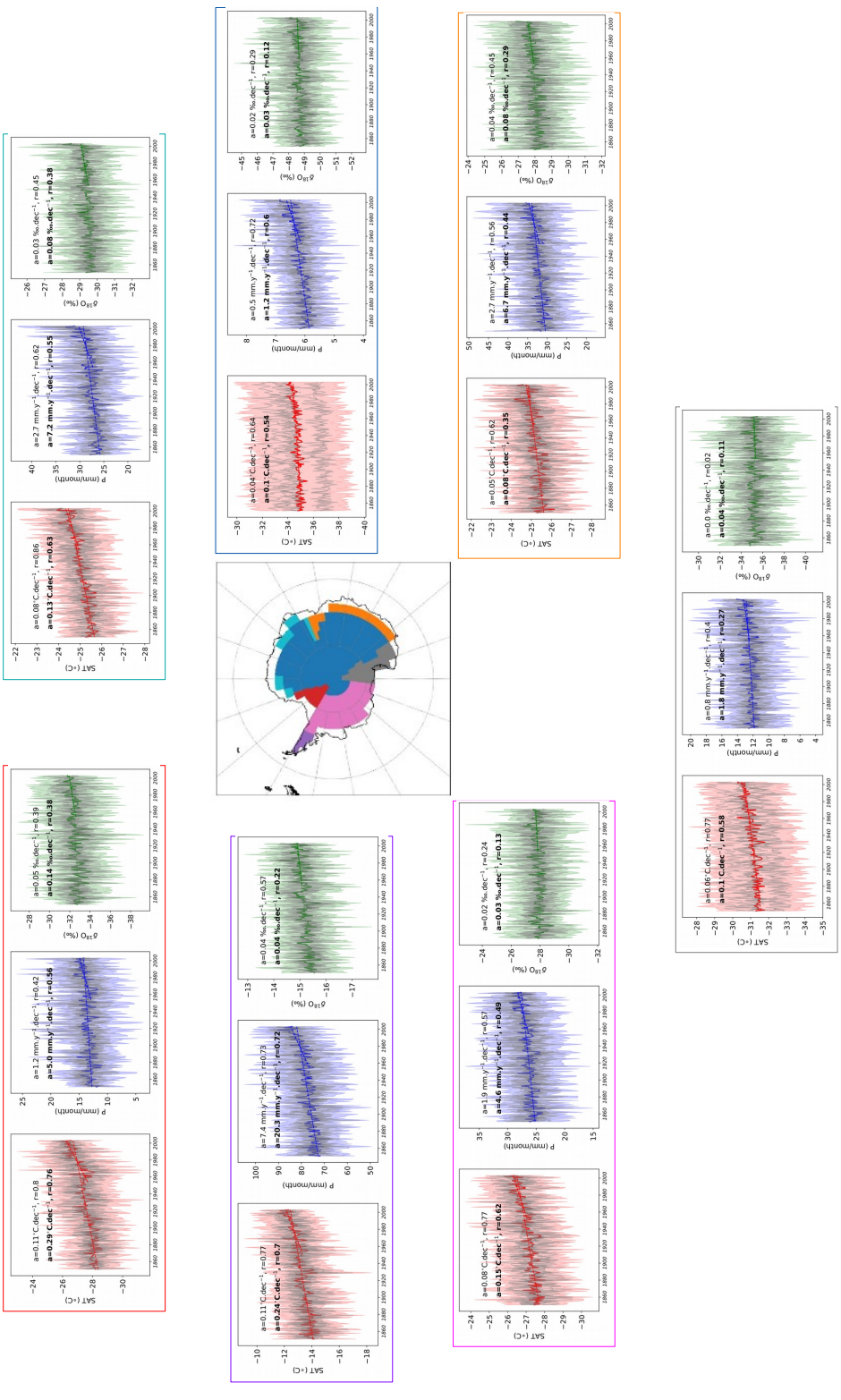

Figure 2. Regional trends over the periods 1851-2005 and 1955-2005. Time series of surface weighted averages of (**A**) surface air temperature ("SAT" in °C, in red), (**B**) precipitation ("P in mm/month", in blue), (**C**) $\delta^{18}O$ (in ‰, in green) and (**D**) sea-ice concentration ("SIC" in %, in grey) over the period 1851–2005, for the different Antarctic regions as defined by (Stenni et al., 2017). Colored solid lines represent the annual average of the ensemble mean, the colored surfaces represent the annual standard deviations of the ensemble mean, the grey solid lines the simulations, and the dashed lines, the linear regressions. The slopes ("a") and the correlation coefficients ("r") are given on the top right of the figures.

https://doi.org/10.5194/egusphere-2023-2735
Preprint. Discussion started: 7 December 2023

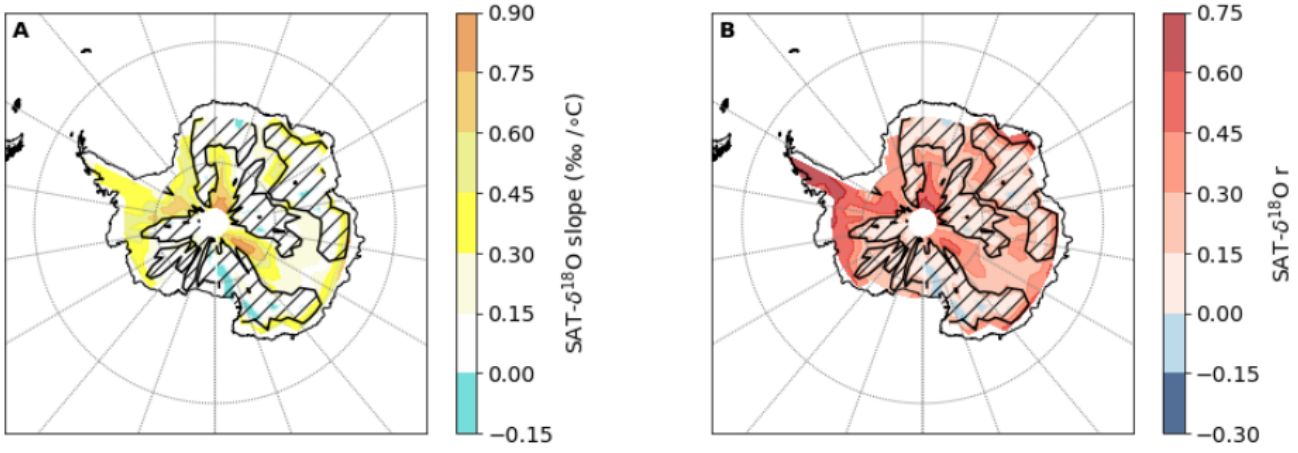

Figure 3. Historical SAT–δ^{18}O pattern. The SAT-δ^{18}O slopes (left panel) and correlation coefficients (right panel) simulated by the HadCM3 over the historical period at the interannual scale at each grid point. Gradients (in ‰/°C, "A") and correlation coefficients ("r") of the SAT–δ^{18}O relationships at the interannual scale (151 points) at each Antarctic grid point and based on the stacked simulations. Regions of hashed black lines indicate to no significant relationships (p-value $\geq$0.05).

https://doi.org/10.5194/egusphere-2023-2735
Preprint. Discussion started: 7 December 2023

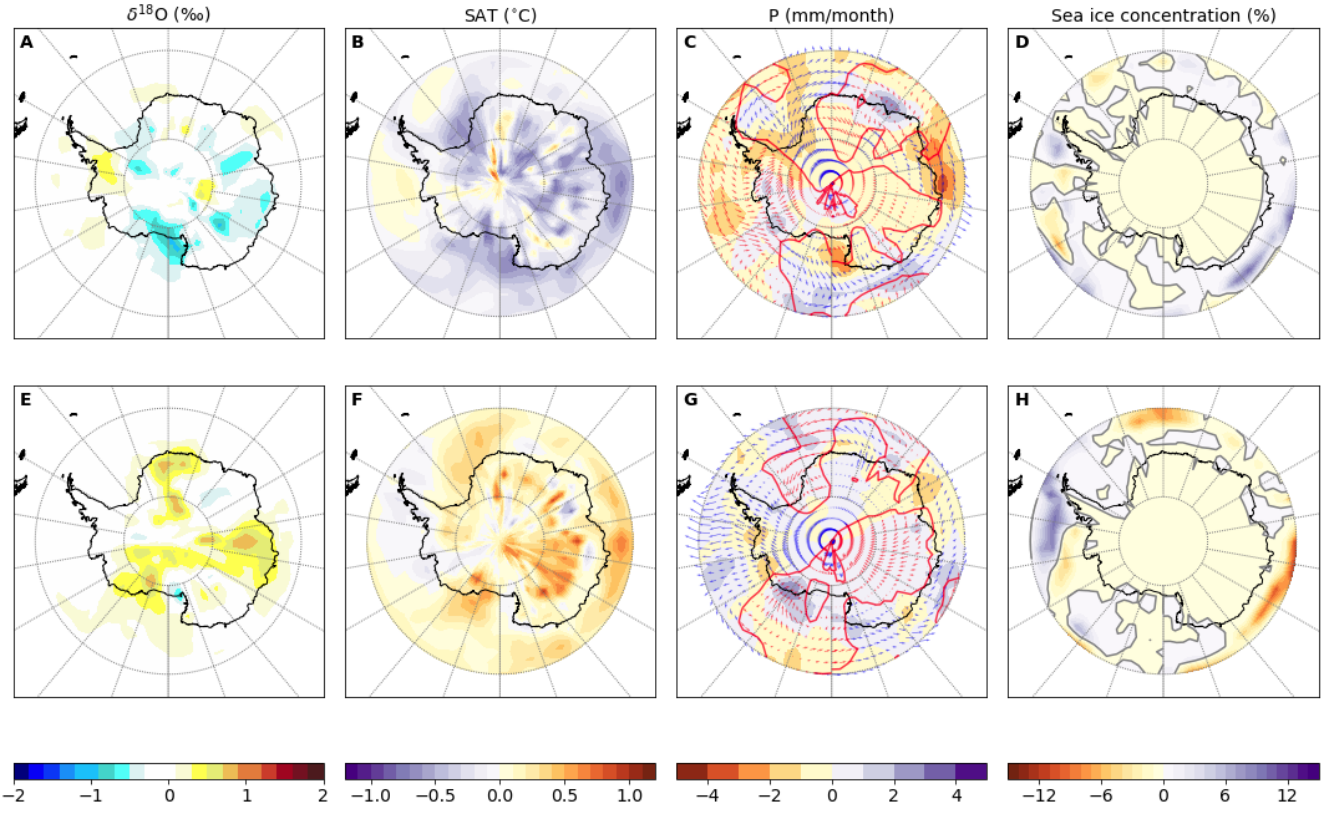

Figure 4. Composite maps for cold (top) and warm (bottom) years. Maps of Antarctic (**A, E**) δ^{18}O (in ‰), (**B, F**) surface air temperature ("SAT" in °C), (**C, G**) precipitation ("P" in mm/month), and (**D, H**) sea-ice concentration ("SIC" in %), for years with surface air temperatures below (top row) and above (bottom row) two standard deviations in the ensemble mean over the period 1851-2004. Maps use the detrended ensemble mean (See Methods). There are 8 years (out of the 155 simulated years) with SAT anomalies out of the plus or minus two standard deviations, 4 are above that range, 4 are below that range. C and G also show the wind field. Blue (red) arrows indicate southward (northward) winds> Regions of the southward winds are delimited using red contours.

https://doi.org/10.5194/egusphere-2023-2735
Preprint. Discussion started: 7 December 2023

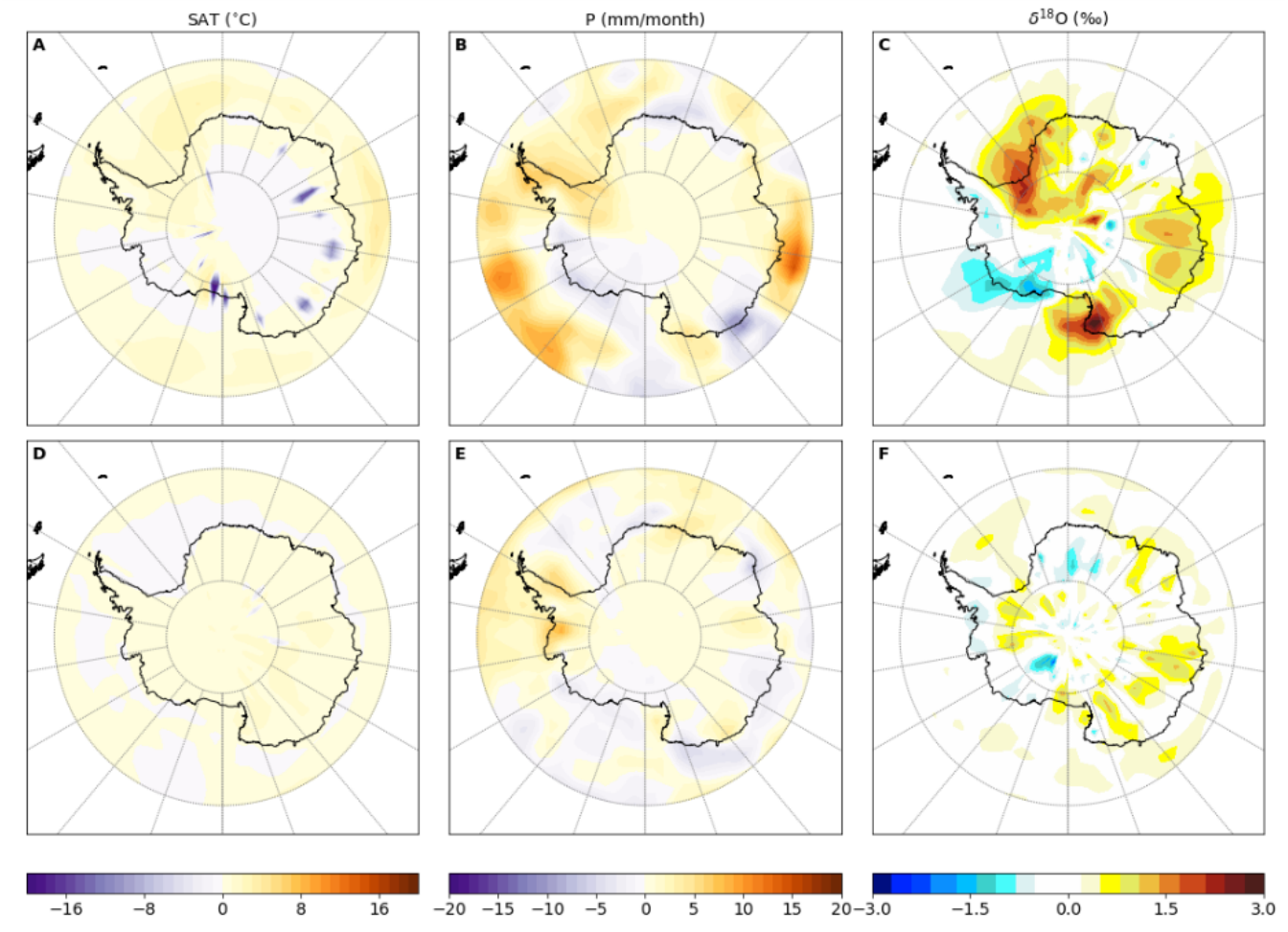

Figure 5. Seasonal Warm-Cold changes. Differences between the warm and cold ensemble means for the winter season (i.e. June to August, **first row: A,B,C**) and the summer season (i.e. from December to February, **second row: D,E,F**), of the surface air temperature (**A,D**, "SAT" in °C), the precipitation (**B,F**, "P" in mm/month), and the precipitated δ^{18}O (**C,F**, "δ^{18}O" in ‰).

https://doi.org/10.5194/egusphere-2023-2735
Preprint. Discussion started: 7 December 2023

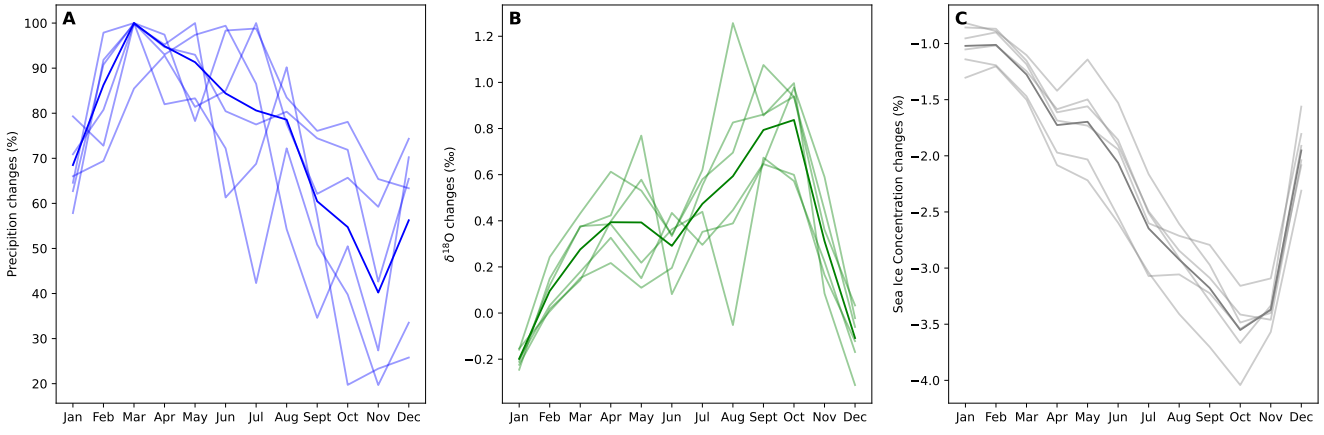

Figure 6. Impact of climate seasonal changes. Seasonal differences of the precipitation (in %), the precipitated δ^{18}O (in ‰) and the sea ice concentration (in %) between the first fifty simulated years and the last fifty simulated years. Light lines correspond to the member simulations and the dark line correspond to the ensemble mean.

https://doi.org/10.5194/egusphere-2023-2735
Preprint. Discussion started: 7 December 2023

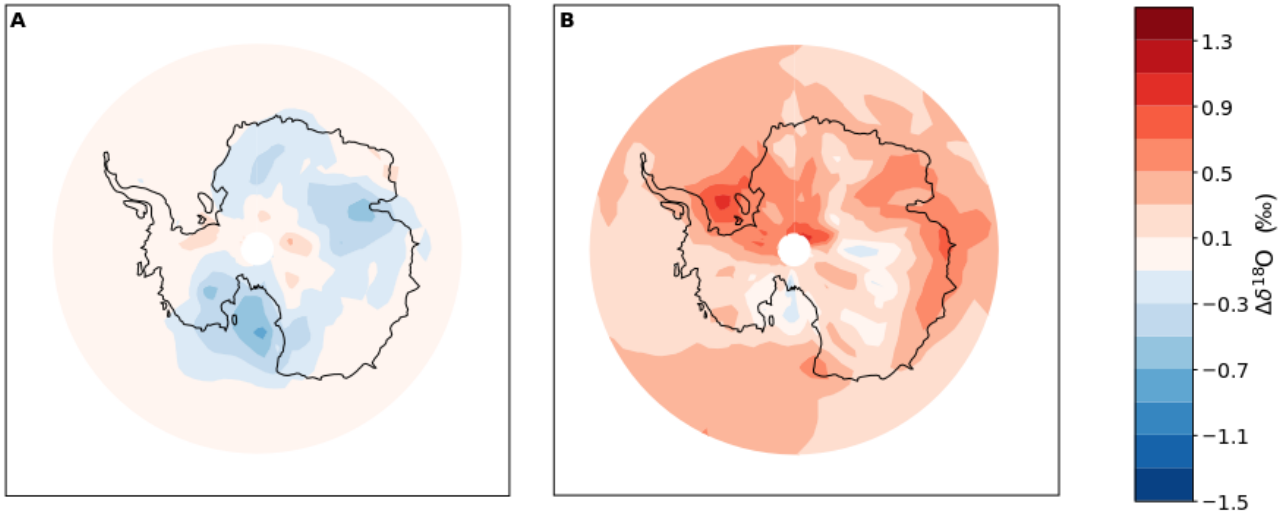

Figure 7. The impact of seasonal changes in the precipitation and on mean annual δ^{18}O on δ^{18}O. δ^{18}O changes ($\Delta\delta^{18}$O in ‰) due to changes in the seasonal cycle of precipitation (A) and due to changes in the seasonal cycle δ^{18}O (B) between the last fifty simulated years and the first fifty simulated years of the HadCM3 historical mean ensemble. See Methods for details of the decomposition.

https://doi.org/10.5194/egusphere-2023-2735
Preprint. Discussion started: 7 December 2023

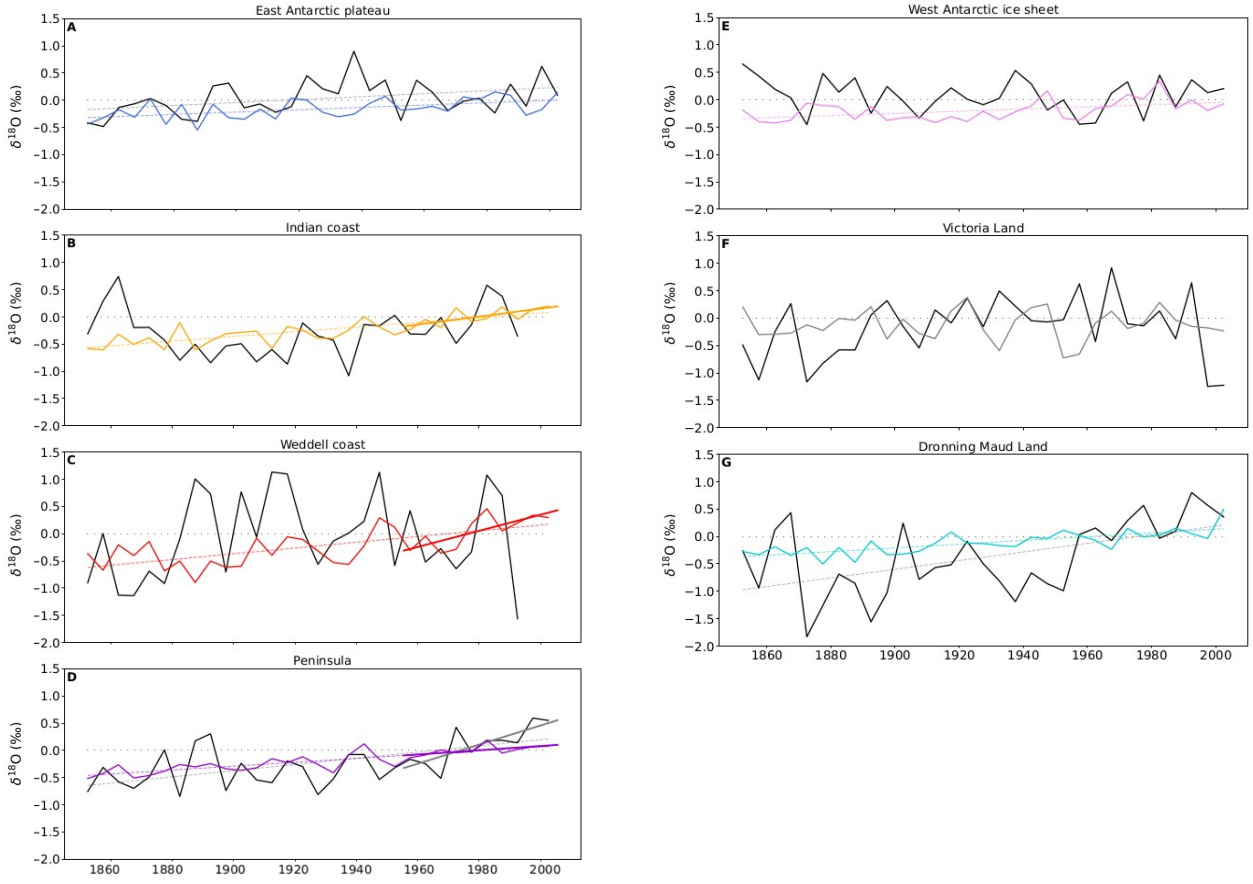

Figure A1. Historical δ^{18}O time series based on 5-years bins from ice core data and HadCM3. Time series of Antarctic surface weighted averages of δ^{18}O (in ‰) based on 5-year bin averages from ice core data (Stenni et al., 2017, black solid lines) and simulated by the HadCM3 model (ensemble mean, colored lines) for each region of Antarctica as defined in the A2k project over the historical period 1851-2004. Dashed lines correspond to linear regressions.

https://doi.org/10.5194/egusphere-2023-2735
Preprint. Discussion started: 7 December 2023

Table A1. Regional surface air temperature trends (in °C/100y): A2k reconstructions over the last 100 years (Stenni et al., 2017) based on the ECHAM5-wiso model and scaled on the climate field reconstruction from (Nicolas and Bromwich, 2014) ('A2k lower bound' and 'A2k upper bound'), as well as the HadCM3 simulated trends over the whole historical period (1851–2004). The relationships are significant.

Region	A2k lower bound	A2k upper bound	HadCM3
Plateau	-1.28	-0.49	0.4
Indian coast	0.47	1.7	0.98
Weddell coast	-0.79	-0.5	0.8
WAIS	0.97	1.33	0.8
Victoria Land	-0.64	-0.55	0.6
Dronning Maud Land	0.98	1.33	1.11

https://doi.org/10.5194/egusphere-2023-2735
Preprint. Discussion started: 7 December 2023

Table B1. Regional sea ice area trends : slope plus or minus the standard error of the slope (in 10^3 km^2/y). The correlation coefficients are given into brackets. Only significant relationships are given. The sea ice regions are defined in term of longitudes as follows: the Indian sector is limited between 20 °E and 90 °E. The Pacific sector is limited between 90 °E and 160 °E. The Ross sector is limited between 160 °E abd 230 °E. The Bellingshausen – Amundsen is limited between 230 °E and 300 °E. Finally the Weddell sector is limited between 300 °E and 20 °E.

Region	Historical	Last 50 years
Indian	-4.9±0.5 (-0.67)	-5.5±2.3 (-0.32)
Pacific	-2.5±0.4 (-0.44)	-4.9±2.0 (-0.33)
Ross	-4.0±0.4 (-0.60)	-8.5±2.0 (-0.33)
Bellingshausen Amundsen	-3.5±0.5 (-0.51)	-7.9±2.5 (-0.41)
Weddell	-2.4±2.4 (-0.64)	–

https://doi.org/10.5194/egusphere-2023-2735
Preprint. Discussion started: 7 December 2023

Table C1. Statistical description of the surface air temperature ("SAT", in °C), precipitation ("Precip", in mm/month) and δ^{18}O (in ‰) for the cold and warm ensembles: minimum ("min"), maximum ("max"), mean ± the standard deviation ("mean±std").

Variable	Cold ensemble			Warm ensemble		
	Min	Max	Mean±Std	Min	Max	Mean±Std
SAT	-1.29	0.85	-0.49±0.36	-0.92	1.39	0.47±0.34
Precip	-4.0	3.4	-0.71±0.77	-3.1	5.8	0.54±0.60
δ^{18}O	-1.94	0.28	-0.62±0.42	-0.07	1.6	0.65±0.33

https://doi.org/10.5194/egusphere-2023-2735
Preprint. Discussion started: 7 December 2023

Table D1. δ^{18}O – SAT gradients in ‰/°C at ice core locations. Gradients are accompanied with the standard error. Correlation coefficients are given into brackets. Finally, numbers in italic correpond to non significant relationships (p>0.05).

Vostok	*0.04±0.04 [0.07]*
Dome F	**0.11±0.05 [0.16]**
EDC	**0.23±0.07 [0.26]**
EDML	*0.01±0.03 [0.04]*
Talos	**-0.09±0.04 [-0.18]**
Taylor Dome	*0.06±0.07 [0.08]*
WDC	**0.10±0.04 [0.2]**
Dome B	*0.07±0.04 [0.13]*
Law Dome	**0.65±0.1 [0.46]**
Siple Dome	*0.08±0.06 [0.12]*
Byrd	*0.07±0.05 [0.12]*
Dome A	*0.04±0.04 [0.12]*
RICE	**0.07±0.03 [0.18]**
Fletcher	**0.21±0.03 [0.54]**
James Ross	**0.25±0.03 [0.58]**
Berkner	**0.49±0.05 [0.64]**
Skytrain	**0.43±0.08 [0.41]**
Hercules Dome	*0.003±0.03 [0.01]*